

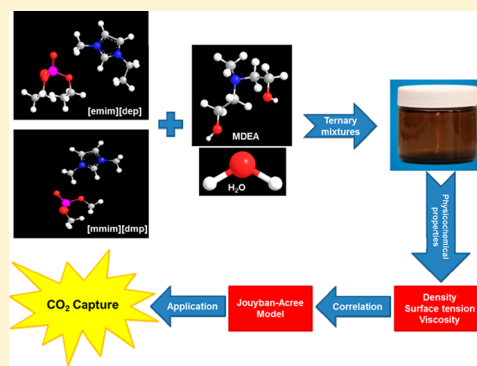
Density, Surface Tension, and Viscosity of Ionic Liquids (1-Ethyl-3-methylimidazolium diethylphosphate and 1,3-Dimethylimidazolium dimethylphosphate) Aqueous Ternary Mixtures with MDEA

Noraini Abd Ghani,[†] Nor Asrina Sairi,^{*,†} Mohamed Kheireddine Aroua,[‡] Yatimah Alias,[†] and Rozita Yusoff[‡]

[†]Chemistry Department, Faculty of Science, University of Malaya, 50603 Kuala Lumpur, Malaysia

[‡]Chemical Engineering Department, Faculty of Engineering, University of Malaya, 50603 Kuala Lumpur, Malaysia

ABSTRACT: The density, surface tension, and viscosity of ionic liquids (1-ethyl-3-methylimidazolium diethylphosphate and 1,3-dimethylimidazolium dimethylphosphate) and ternary mixtures with aqueous MDEA, were measured over the whole concentrations range at various temperatures (293.15–343.15) K by using Anton Paar DMA 4500 densimeter, Kruss Processor Tensiometer K100, and R/S+ Brookfield rheometer. The experimental density and surface tension decrease linearly with mole fractions of ionic liquids. Data on viscosity demonstrates a temperature-dependence behavior, that decreased nonlinearly with temperature. Evaluations of the measured physicochemical properties were completed. The best correlation for density and surface tension data were linear fitting, while the viscosity data was obtained by polynomial regression. ILs mole fraction also influenced the experimental density, surface tension, and viscosity. The Jouyban–Acree model was used to correlate the physicochemical properties of the mixtures and pure compounds at different temperatures. The absolute percentage error (APER) for each correlations was less than 8 %, proving that this model accurately represents the physicochemical properties data.



1. INTRODUCTION

In recent years, the capture of CO₂ from flue gas has gained a lot of interests by manufacturers due to international efforts for the reduction of greenhouse gas emissions. Capturing of CO₂ from flue gas presents an additional challenge, even though CO₂ separation processes have been extensively utilized in industry.¹ Various CO₂ capture technologies have received widespread attention particularly physical absorption,^{2,3} chemical absorption,^{4,5} and adsorption.^{6,7} Meanwhile, in screening feasible ILs in capturing CO₂, many factors have to be considered such as cost, stability, corrosiveness, toxicity, and environmental impact.^{8,9} Ionic liquids (ILs) with dialkylphosphate anions are biodegradable, less toxic, and greener than other ILs⁸ and probable for practical applications because they can be produced in a one-pot reactor under mild conditions with very high yield.⁹

Chemical absorption with aqueous alkanolamine is the most appropriate for CO₂ capture.⁴ However, there are some drawbacks which negatively affect the technology efficiency such as high equipment corrosion rate, high energy consumption, and a large absorber volume needed.¹⁰ Thus, ILs with methyldiethanolamine (MDEA) aqueous mixtures have been introduced to overcome these weaknesses.

The application of ILs for CO₂ uptake was improved by blending ILs with mixed amines such as MDEA aqueous solution. Consequently, the addition of ILs increased the CO₂ absorption rate and decreased the vapor pressure of amines.¹¹ Zhang et al.¹² successfully found functionalized ILs with MDEA

aqueous solutions had high CO₂ absorption rate and large uptake capacity. The ILs with MDEA aqueous solutions were more suitable for the industrial device than pure IL.¹¹ High concentrated aqueous solutions of IL–MDEA with high temperature are efficient for the absorption under low pressure; meanwhile, a lower temperature is recommended for high pressure absorption.¹³ However, Ahmady et al.¹⁴ reported that all used ILs in their research reduced the CO₂ loading in aqueous MDEA solutions. The CO₂ loading in all IL+MDEA mixtures increases with increasing CO₂ partial pressure and decreases with increasing temperature.

The determination of physicochemical properties of a substance is crucially important in the design of various physical and chemical processes,^{15,16} especially for ILs aqueous mixtures. ILs have an excellent ability to replace organic solvents in chemical processes.^{17,18} However, further research remains to be completed in consideration of achieving the precise physicochemical characterization of ILs mixture systems.¹⁹ Therefore, various physicochemical properties of ILs have been studied such as density,^{16,19–21} surface tension,²² and viscosity.²⁰

Ternary mixtures of organic solvent–IL–water system have been studied to achieve lower viscosity of solution, which directly lower energy requirements for absorption processes of CO₂.^{23,24}

Received: June 17, 2013

Accepted: May 12, 2014

Knowledge of interface properties, especially the surface and interfacial tension, and its relationship to the ILs chemical nature is crucial to choose the right IL for a specific application.²² In this study, physical properties of ternary system MDEA–IL–water for density, surface tension, and viscosity are reported.

2. EXPERIMENTAL SECTIONS

2.1. Chemicals. 1-Ethyl-3-methylimidazolium diethylphosphate ([emim][dep], minimum mass purity $\geq 98\%$), 1,3-dimethylimidazolium dimethylphosphate ([mmim][dmp], minimum mass purity $\geq 98\%$) and pure *N*-methyldiethanolamine (MDEA, purity $\geq 98\%$) were purchased from Merck. All chemicals were of analytical grade and used without further purification.

2.2. Sample Preparation. Different mole fractions for aqueous ternary mixtures of [emim][dep]-MDEA-H₂O and [mmim][dmp]-MDEA-H₂O, systems were prepared as tabulated in Table 1.

Table 1. Compositions of ILs, MDEA, and water in Ternary Mixtures^a

system	mole fraction		
	X_{IL}	X_{MDEA}	$X_{\text{H}_2\text{O}}$
(i) [emim][dep] + MDEA + H ₂ O			
0.1	0.0986	0.1944	0.7070
0.2	0.2091	0.5412	0.2497
0.3	0.3666	0.3676	0.2658
0.4	0.4188	0.2162	0.3650
0.6	0.5973	0.2911	0.1116
0.7	0.6825	0.2899	0.0276
0.8	0.8097	0.1903	0.0000
0.9	0.9134	0.0866	0.0000
1	1.0000	0.0000	0.0000
(ii) [mmim][dmp] + MDEA + H ₂ O			
0.1	0.0774	0.2789	0.6438
0.2	0.1998	0.4346	0.3657
0.3	0.3247	0.6054	0.0699
0.4	0.3753	0.3888	0.2359
0.5	0.4772	0.2393	0.2835
0.6	0.6367	0.3295	0.0338
0.7	0.6866	0.3126	0.0008
0.8	0.8238	0.1565	0.0197
0.9	0.9305	0.0695	0.0000
1	1.0000	0.0000	0.0000

^aStandard uncertainties, u are $u(T) = 0.01$ K, $u(x) = 0.0001$, and $u(P) = 1$ kPa.

2.3. Apparatus and Procedure. *Density.* Density measurement of the aqueous ternary mixtures was carried out with densimeter DMA 4500 (Anton Paar, Austria) at various temperature [(293.15 to 343.15) K]. The apparatus is precise within $1.0 \cdot 10^{-4}$ g·cm⁻³, and the expanded uncertainty of the measurements was estimated to be better than 0.001 g·cm⁻³. Calibration of the densitometer was performed at atmospheric pressure using dry air and pure water (supplied).

Surface Tension. Surface tension measurement was carried out using KRÜSS Processor Tensiometer K100 using Du Noüy ring method in various temperatures from (293.15 to 343.15) K. The tensiometer has a surface tension range of (1–1000) mN·m⁻¹ with 0.01 resolutions. The instrument is equipped with a maximum temperature range of 403.15 K and a minimum of

263.15 K. In general, each surface tension value reported was an average of ten measurements. Calibration of the tensiometer was performed by determining the surface tensions of distilled water and pure MDEA and comparing with literature data.

Viscosity. As for the viscosity study, concentrations for aqueous ternary systems of ILs range from (0.1 to 1.0) M were determined. The viscosity measurements were carried out using R/S+ rheometer (Brookfield, USA). The rheometer is a controlled stress (or controlled torque) instrument and was calibrated using standard viscosity oil. Temperature of the solution was maintained within ± 0.1 K. The viscosity was measured with an accuracy less than 3 %. All measurements for each sample were performed in triplicate, and the values were reported as an average. The measurement was taken at atmospheric pressure and temperature range between (293.15 and 343.15) K, with 10 K increment.

3. RESULTS AND DISCUSSION

The validation of data using MDEA was carried out to ensure the accuracy of measurement used in this work. These experimental data of pure compound and comparisons with the literature reviews^{24–28} were presented in Table 2.

Table 2. Comparison of Measured Densities, Surface Tensions, and Viscosities with Literature Values for MDEA Pure Components at 0.1 MPa^a

T/K	density, ρ /g·cm ⁻³		surface tension, γ /mN·m ⁻¹		viscosity, η /mPa·s	
	exptl.	lit.	exptl.	lit.	exptl.	lit.
303.15	1.0338	1.03356 ^b 1.03410 ^c	37.33	37.29 ^d 37.31 ^e	56.3000	57.50 ^b 57.57 ^f
313.15	1.0267	1.02640 ^b 1.02652 ^c		N/A	34.4474	35.00 ^b 34.78 ^f
323.15	1.0189	1.01901 ^b 1.01887 ^c		N/A	22.9255	22.00 ^b 21.98 ^f
333.15		N/A	35.47	35.58 ^d	14.9923	N/A

^aStandard uncertainties, u are $u(T) = 0.01$ K, $u(x) = 0.0001$, $u(P) = 1$ kPa and $u(\gamma) = 0.15$ mN·m⁻¹. Relative standard uncertainties, u_r are $u_r(\rho) = 0.001$ and $u_r(\eta) = 0.03$. ^bData from ref 22. ^cData from ref 24. ^dData from ref 23. ^eData from ref 25. ^fData from ref 26.

The measured densities, ρ , surface tensions, γ and viscosities, η for the aqueous ternary mixtures of [emim][dep] and [mmim][dmp] with MDEA at $T = (293.15, 301.15, 303.15, 313.15, 323.15, 333.15, \text{ and } 343.15)$ K over the whole composition range are listed in Tables 3 and 4.

Density. Figures 1 and 2 present the experimental densities of ternary mixtures of [emim][dep] and [mmim][dmp] with MDEA. The findings indicate that ILs ternary mixtures demonstrate temperature-dependence behavior and liquid density decreases linearly with temperature increment. The density of all the compositions always increases with the ILs mole fractions, and decreases with temperature, in agreement with Ciocirlan and co-workers.²⁹

The accuracy of the density data were further evaluated by correlation with temperature either by linear, exponential, power or polynomial equations. The best correlation was obtained by linear equation ($R^2 = 0.99$). Soriano et al.³⁰ and Jacquemin et al.³¹ also reported the linear behavior with temperature being for pure ILs.

Figures 3 and 4 present the experimental densities of ternary mixtures of [emim][dep] and [mmim][dmp] with MDEA in different temperature as a function of mole fraction. It is obvious

Table 3. Experimental Densities (ρ), Surface Tensions (γ), and Viscosities (η) for Ternary Mixtures at Different Temperatures for [emim][dep]–MDEA–H₂O at 0.1 MPa^a

	T/K	293.15	301.15	303.15	313.15	323.15	333.15	343.15
	X _i							
[emim][dep]–MDEA–H ₂ O								
ρ/g·cm ^{−3}	0.1	1.0912	1.0837	1.0815	1.0723	1.0623	1.0501	1.0348
	0.2	1.1004	1.0933	1.0913	1.0814	1.0721	1.0597	1.0438
	0.3	1.1145	1.1074	1.1058	1.0966	1.0863	1.0744	1.0594
	0.4	1.1230	1.1163	1.1142	1.1051	1.0960	1.0846	1.0689
	0.6	1.1290	1.1223	1.1201	1.1124	1.1031	1.0920	1.0768
	0.7	1.1353	1.1287	1.1269	1.1191	1.1101	1.0987	1.0817
	0.8	1.1399	1.1331	1.1314	1.1238	1.1147	1.1034	1.0878
	0.9	1.1460	1.1388	1.1369	1.1292	1.1201	1.1086	1.0923
	1.0	1.1530	1.1452	1.1429	1.1343	1.1245	1.1134	1.0977
γ/mN·m ^{−1}	0.1	37.61	37.41	37.36	37.15	36.94	36.78	36.63
	0.2	37.21	37.05	37.01	36.81	36.62	36.47	36.29
	0.3	36.52	36.35	36.31	36.13	35.91	35.68	35.47
	0.4	36.31	36.13	36.09	35.89	35.69	35.48	35.25
	0.6	36.01	35.85	35.81	35.62	35.42	35.24	35.05
	0.7	35.76	35.63	35.60	35.42	35.24	35.08	34.89
	0.8	35.58	35.45	35.41	35.25	35.08	34.91	34.72
	0.9	35.43	35.30	35.26	35.12	34.96	34.78	34.57
	1.0	35.29	35.15	35.12	34.98	34.83	34.64	34.43
η/mPa·s	0.1	41.4339	29.6484	27.0616	17.8278	12.1118	8.7245	6.5644
	0.2	72.0000	52.3037	48.2755	31.9723	22.5031	17.8281	13.5040
	0.3	96.8000	67.1318	63.1407	40.2889	25.6371	19.2430	14.0211
	0.4	114.3000	78.1407	69.6294	48.3817	32.2020	23.7283	16.3701
	0.6	165.3006	112.7113	103.4241	68.0464	42.3307	28.1679	21.6359
	0.7	207.5924	135.2498	120.1645	75.7333	52.2512	35.6182	26.9558
	0.8	258.1360	162.8320	141.8077	81.9080	55.5458	38.8716	23.6362
	0.9	327.8395	201.5538	180.5538	100.5176	61.2818	41.3168	28.5453
	1.0	577.2231	320.2527	281.2820	151.9150	89.0253	58.1505	40.1934

^aStandard uncertainties, u , are $u(T) = 0.01$ K, $u(x) = 0.0001$, and $u(P) = 1$ kPa, and $u(\gamma) = 0.15$ mN·m^{−1}. Relative standard uncertainties, u_r , are $u_r(\rho) = 0.001$ and $u_r(\eta) = 0.03$.

that the density increases with increasing of mole fraction of ILs. The density of [emim][dep] mixture is less denser compare to [mmim][dmp] mixture. This is in agreement with Pinkert et al.³² that larger ions result in less denser ILs. We found no previous data as a function of mole fraction for [emim][dep] or [mmim][dmp] or their mixtures with water.

Surface Tension. Figures 5 and 6 show the effects of temperature and composition on surface tension of ternary mixtures of [emim][dep] and [mmim][dmp] with MDEA. To establish the accuracy of the experimental data obtained in this work, surface tension of pure MDEA was determined at (313.15 and 333.15) K, and compare with literature^{25,27} which were tabulated in Table 2.

Surface tensions for the whole compositions of aqueous ternary mixtures were obtained at (293.15, 301.15, 303.15, 313.15, 323.15, 333.15, and 343.15) K. The surface tension results are given in Tables 3 and 4 and plotted as a function of temperature in Figures 5 and 6. It is observed that the surface tension results show a linear dependence with a temperature in the composition (mole fractions) considered. The accuracy of the surface tensions data was further assessed by correlating them with temperature by means of a linear equation, resulted good correlations ($R^2 = 0.99$). A linear variation of surface tension with temperature for ionic liquid is in agreement with Wang et al.³³

Figures 7 and 8 present the surface tension of ternary mixtures of [emim][dep] with MDEA and [mmim][dmp] with

MDEA in different temperature as a function of mole fraction. Ternary mixtures of [emim][dep] with MDEA have lower surface tension than ternary mixtures of [mmim][dmp] with MDEA. This is in agreement with Tariq et al.,³⁴ who reported the surface tension of the mixtures depends strongly on the alkyl chain length of the ILs. ILs with longer alkyl chains producing mixtures with lower surface tension values at any given composition. Surface tension of [emim][dep] mixture is lower than [mmim][dmp] mixture which have longer alkyl chains.

The surface tension decreases with the increasing of ILs mole fraction for [emim][dep]–MDEA–H₂O. However, the surface tension increases with the decreasing of ILs mole fraction for [mmim][dmp], probably because of high energy binding of [emim][dep] compared to [mmim][dmp]. The surface tensions for these ILs decrease proportionately as the alkyl chain size increases, which are related to the anion influence.³⁵

Viscosity. The result of density measurements at the temperature range from (293.15 to 343.15) K of aqueous ternary mixtures of [emim][dep] with MDEA and [mmim][dmp] with MDEA are summarized in Tables 2 and 3. As expected, for every measured composition of ternary mixtures, the viscosity decreases with increasing temperature. Nevertheless, this decrease is considerably greater than densities³⁶ and surface tensions data. In Figures 9 and 10, the results indicate that viscosity of ternary mixtures demonstrate temperature-dependence behavior, reveals the viscosities are more influenced by temperature,²⁹ which decreases nonlinearly with temperature.

Table 4. Experimental Densities (ρ), Surface Tensions (γ), and Viscosities (η) for Ternary Mixtures at Different Temperatures for [mmim][dmp]–MDEA–H₂O at 0.1 MPa^a

	T/K	293.15	301.15	303.15	313.15	323.15	333.15	343.15
	X_i							
[mmim][dmp]–MDEA–H ₂ O								
$\rho/\text{g}\cdot\text{cm}^{-3}$	0.1	1.1071	1.1006	1.0986	1.0919	1.0852	1.0766	1.0663
	0.2	1.1284	1.1221	1.1207	1.1124	1.1049	1.0958	1.0829
	0.3	1.1486	1.1421	1.1401	1.1295	1.1201	1.1088	1.0967
	0.4	1.1673	1.1606	1.1587	1.1481	1.1396	1.1287	1.1145
	0.5	1.1863	1.1799	1.1778	1.1683	1.1602	1.1489	1.1367
	0.6	1.2048	1.1971	1.1948	1.1871	1.1793	1.1689	1.1561
	0.7	1.2185	1.2109	1.2091	1.1996	1.1918	1.1813	1.1691
	0.8	1.2398	1.2336	1.2321	1.2238	1.2157	1.2052	1.1915
	0.9	1.2473	1.2408	1.2392	1.2313	1.2226	1.2120	1.1987
	1.0	1.2525	1.2461	1.2441	1.2368	1.2274	1.2172	1.2034
$\gamma/\text{mN}\cdot\text{m}^{-1}$	0.1	40.43	40.29	40.24	40.01	39.75	39.38	39.04
	0.2	40.97	40.82	40.79	40.58	40.34	39.96	39.60
	0.3	41.97	41.75	41.68	41.41	41.08	40.69	40.33
	0.4	42.97	42.71	42.63	42.35	42.01	41.58	41.21
	0.5	43.59	43.28	43.19	42.85	42.55	42.13	41.72
	0.6	44.16	43.91	43.82	43.53	43.21	42.78	42.39
	0.7	44.76	44.41	44.32	43.93	43.56	43.15	42.81
	0.8	45.24	44.94	44.85	44.45	43.98	43.61	43.25
	0.9	45.77	45.52	45.44	45.06	44.63	44.26	43.86
	1.0	46.23	45.95	45.87	45.56	45.12	44.81	44.45
$\eta/\text{mPa}\cdot\text{s}$	0.1	46.6395	29.1966	25.2690	16.4867	11.4700	8.2360	6.9800
	0.2	85.6484	53.8526	48.4783	30.1093	20.4690	13.8367	10.6540
	0.3	94.1090	61.7733	55.8309	35.5910	25.4991	17.2703	13.2983
	0.4	105.8037	69.8091	62.4302	40.4197	27.7074	19.0643	14.1079
	0.5	121.8330	81.3819	73.5440	46.1001	32.5985	22.8632	16.4012
	0.6	149.4780	99.8808	91.1669	58.8255	40.4290	27.9771	20.2820
	0.7	163.3437	109.6022	99.7410	63.1879	41.3600	28.9264	21.1065
	0.8	180.3391	117.9302	106.8806	68.5343	42.3108	30.9817	21.7677
	0.9	202.5040	128.0987	115.2849	72.2165	45.1552	30.3650	22.1353
	1.0	229.5487	138.7974	121.6571	77.6727	47.2535	33.6860	23.9578

^aStandard uncertainties, u_i are $u(T) = 0.01$ K, $u(x) = 0.0001$, and $u(P) = 1$ kPa and $u(\gamma) = 0.15$ mN·m^{−1}. Relative standard uncertainties, u_r are $u_r(\rho) = 0.001$ and $u_r(\eta) = 0.03$.

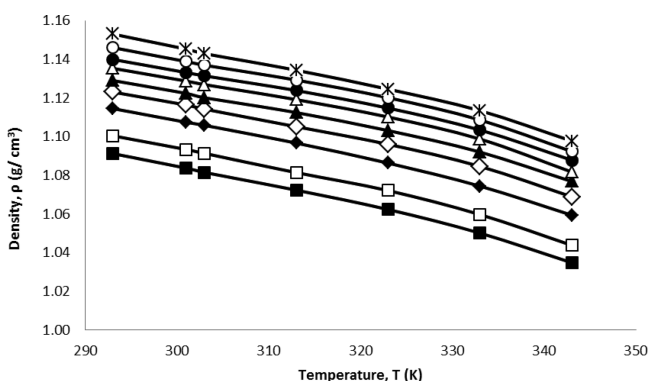


Figure 1. Experimental densities, ρ , of ternary mixtures [emim][dep]–MDEA–H₂O at different mole fractions as a function of temperature. ■, 0.1 X_{IL} ; □, 0.2 X_{IL} ; ◆, 0.3 X_{IL} ; ◇, 0.4 X_{IL} ; ▲, 0.6 X_{IL} ; △, 0.7 X_{IL} ; ○, 0.8 X_{IL} ; ●, 0.9 X_{IL} ; *, 1.0 X_{IL} .

The accuracy evaluation was done by correlating the results with temperature, and the best correlation was obtained with polynomial equation ($R^2 = 0.99$). The results corresponding to Baroutian et al.³⁷ in measurement of physicochemical properties of binary and ternary blends of palm oil + palm biodiesel + diesel fuel at different temperature.

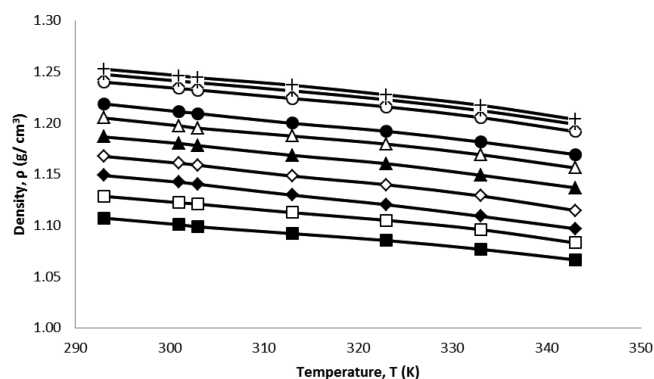


Figure 2. Experimental densities, ρ , of the ternary mixtures [mmim][dmp]–MDEA–H₂O at different mole fractions as a function of temperature. ■, 0.1 X_{IL} ; □, 0.2 X_{IL} ; ◆, 0.3 X_{IL} ; ◇, 0.4 X_{IL} ; ▲, 0.5 X_{IL} ; △, 0.6 X_{IL} ; ○, 0.7 X_{IL} ; ●, 0.8 X_{IL} ; +, 0.9 X_{IL} ; *, 1.0 X_{IL} .

Figures 11 and 12 present the viscosity of ternary mixtures of [emim][dep] with MDEA and [mmim][dmp] with MDEA at different temperatures as a function of mole fraction. At lower ILs mole fraction, viscosity significantly lower, however the value were noticeable at higher mole fraction of ILs. The observation in decrease of viscosity with an increasing of MDEA and water

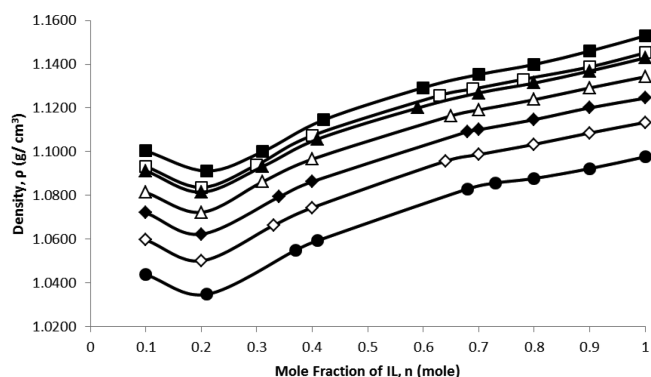


Figure 3. Experimental densities, ρ , of ternary mixtures [emim][dep]-MDEA-H₂O at different temperature as a function of mole fractions. ■, 293.15 K; □, 301.15 K; ▲, 303.15 K; △, 313.15 K; ◆, 323.15 K; ◇, 333.15 K; ●, 343.15 K.

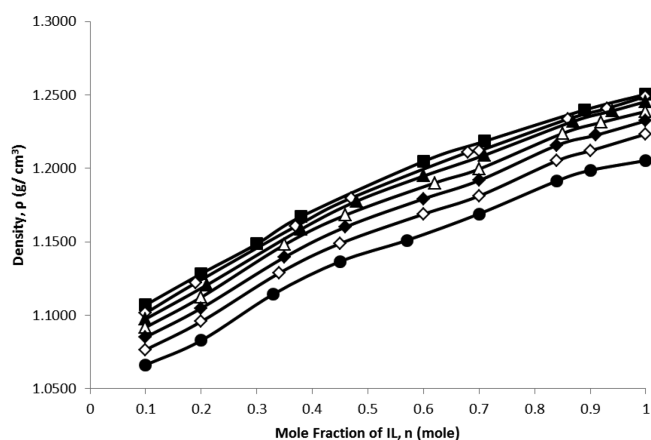


Figure 4. Experimental densities, ρ , of the ternary mixtures [mmim][dmp]-MDEA-H₂O at different temperatures as a function of mole fractions. ■, 293.15 K; □, 301.15 K; ▲, 303.15 K; △, 313.15 K; ◆, 323.15 K; ◇, 333.15 K; ●, 343.15 K.

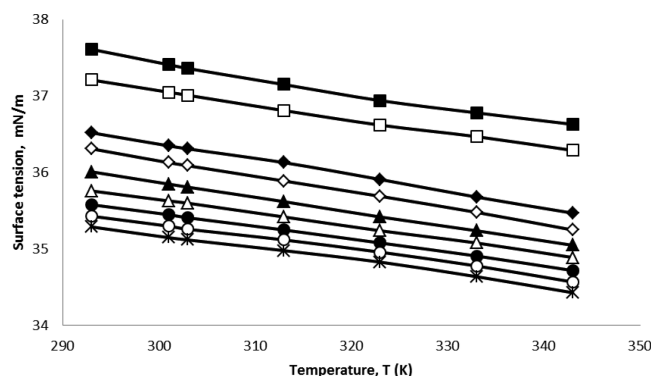


Figure 5. Experimental surface tension, γ , of ternary mixtures [emim][dep]-MDEA-H₂O at different mole fractions as a function of temperature. ■, 0.1 X_{IL} ; □, 0.2 X_{IL} ; ◆, 0.3 X_{IL} ; ◇, 0.4 X_{IL} ; ▲, 0.5 X_{IL} ; △, 0.6 X_{IL} ; ○, 0.7 X_{IL} ; ●, 0.8 X_{IL} ; *, 0.9 X_{IL} ; +, 1.0 X_{IL} .

content is particularly strong in dilute solutions in ILs mixture. Ion-dipole interactions and/or hydrogen bonding between the cation of the IL and water will take place. Conclusively, this weakening of the strong hydrogen bonding interactions between the cation and anion of the IL leads to a higher mobility of the ions and a lower viscosity of the mixture.³⁸

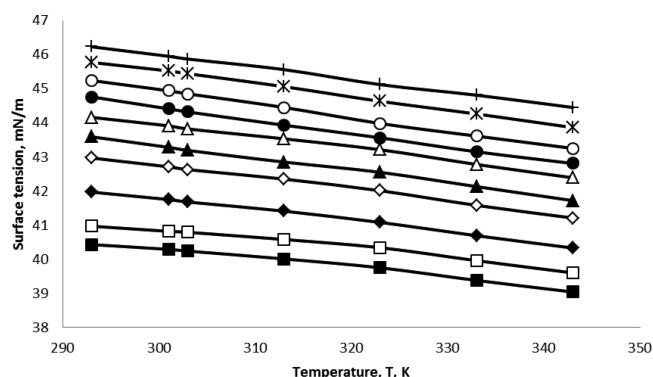


Figure 6. Experimental surface tension, γ , of the ternary mixtures [mmim][dmp]-MDEA-H₂O at different mole fractions as a function of temperature. ■, 0.1 X_{IL} ; □, 0.2 X_{IL} ; ◆, 0.3 X_{IL} ; ◇, 0.4 X_{IL} ; ▲, 0.5 X_{IL} ; △, 0.6 X_{IL} ; ○, 0.7 X_{IL} ; ●, 0.8 X_{IL} ; *, 0.9 X_{IL} ; +, 1.0 X_{IL} .

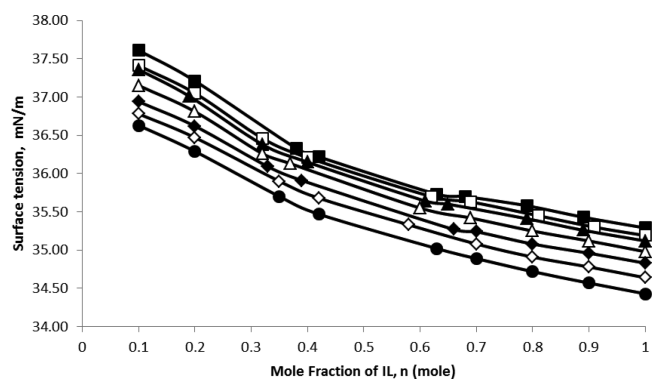


Figure 7. Experimental surface tension, γ , of ternary mixtures [emim][dep]-MDEA-H₂O at different temperatures as a function of mole fractions. ■, 293.15 K; □, 301.15 K; ▲, 303.15 K; △, 313.15 K; ◆, 323.15 K; ◇, 333.15 K; ●, 343.15 K.

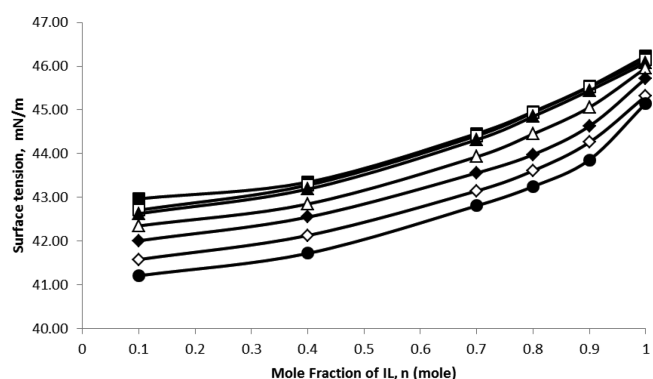


Figure 8. Experimental surface tension, γ , of ternary mixtures [mmim][dmp]-MDEA-H₂O at different temperatures as a function of mole fractions. ■, 293.15 K; □, 301.15 K; ▲, 303.15 K; △, 313.15 K; ◆, 323.15 K; ◇, 333.15 K; ●, 343.15 K.

Figure 13 shows the comparison of the surface tension data between mixtures [emim][dep]-MDEA-H₂O and MEA-MDEA-H₂O³⁹ at different mole fractions as a function of temperature. The similarities in the decreasing of surface tension data between the series were observed. Fu et al.,³⁹ who reported that the increase of CO₂ loading tends to increase the surface tensions at given amine concentration for the CO₂ loaded MEA-MDEA aqueous solutions.

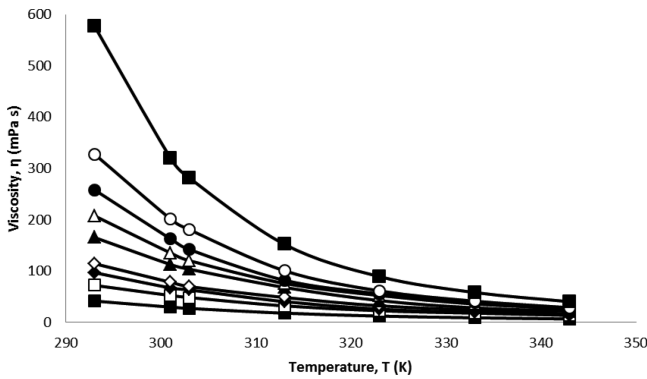


Figure 9. Experimental viscosities, η , of ternary mixtures [emim][dep]-MDEA-H₂O at different mole fractions as a function of temperature. ■, 0.1 X_{IL} ; □, 0.2 X_{IL} ; ◆, 0.3 X_{IL} ; ◇, 0.4 X_{IL} ; ▲, 0.6 X_{IL} ; △, 0.7 X_{IL} ; ○, 0.8 X_{IL} ; ●, 0.9 X_{IL} ; *, 1.0 X_{IL} .

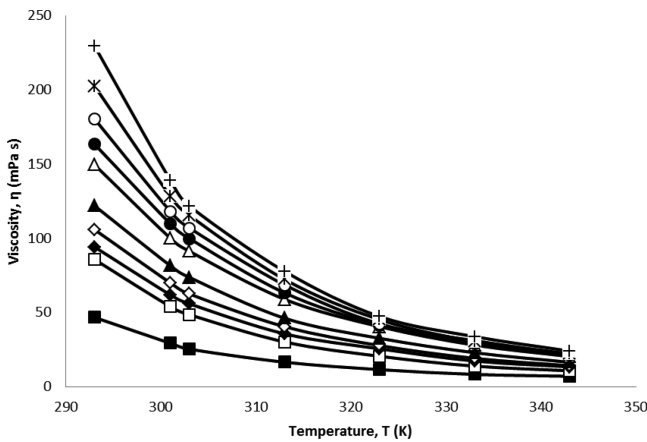


Figure 10. Experimental viscosities, η , of the ternary mixtures [mmim][dmp]-MDEA-H₂O at different mole fractions as a function of temperature. ■, 0.1 X_{IL} ; □, 0.2 X_{IL} ; ◆, 0.3 X_{IL} ; ◇, 0.4 X_{IL} ; ▲, 0.5 X_{IL} ; △, 0.6 X_{IL} ; ○, 0.7 X_{IL} ; ●, 0.8 X_{IL} ; *, 0.9 X_{IL} ; +, 1.0 X_{IL} .

Data Correlation Using the Jouyban-Acree Model.

Density. The Jouyban-Acree model for representing the density of ternary solvents is

$$\begin{aligned} \ln \rho_{m,T} = & x_1 \ln \rho_{1,T} + x_2 \ln \rho_{2,T} + x_3 \ln \rho_{3,T} \\ & + x_1 x_2 \sum_{j=0}^2 \left[\frac{A_j (x_1 - x_2)^j}{T} \right] + x_1 x_3 \\ & \times \sum_{j=0}^2 \left[\frac{B_j (x_1 - x_3)^j}{T} \right] + x_2 x_3 \sum_{j=0}^2 \left[\frac{C_j (x_2 - x_3)^j}{T} \right] \\ & + x_1 x_2 x_3 \sum_{j=0}^2 \left[\frac{D_j (x_1 - x_2 - x_3)^j}{T} \right] \end{aligned} \quad (1)$$

where $\rho_{m,T}$, $\rho_{1,T}$, $\rho_{2,T}$, and $\rho_{3,T}$ are the densities of the mixture and solvents 1, 2, and 3 at temperature T , respectively, and D_j represent the model constants.^{40,41} These model constants are computed by regressing $(\ln \rho_{m,T} - x_1 \ln \rho_{1,T} - x_2 \ln \rho_{2,T} - x_3 \ln \rho_{3,T})$ against $x_1 x_2 / T$, $x_1 x_2 (x_1 - x_2) / T$, $x_1 x_2 (x_1 - x_2)^2 / T$, $x_1 x_3 / T$, $x_1 x_3 (x_1 - x_3) / T$, $x_1 x_3 (x_1 - x_3)^2 / T$, $x_2 x_3 / T$, $x_2 x_3 (x_2 - x_3) / T$, $x_2 x_3 (x_2 - x_3)^2 / T$, $x_1 x_2 x_3 / T$, $x_1 x_2 x_3 (x_1 - x_2 - x_3) / T$, and $x_1 x_2 x_3 (x_1 - x_2 - x_3)^2 / T$ using a no intercept least-squares

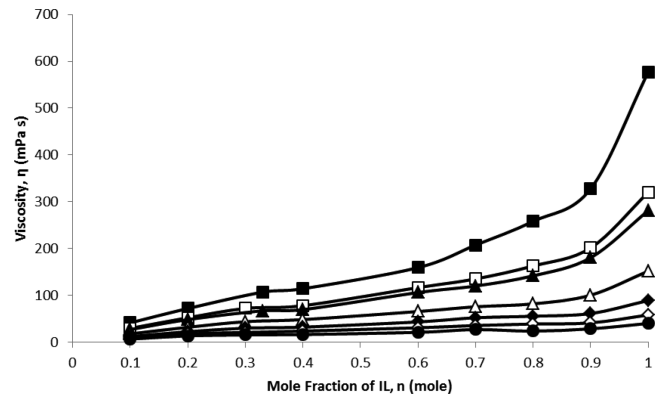


Figure 11. Experimental viscosities, η , of ternary mixtures [emim][dep]-MDEA-H₂O at different temperatures as a function of mole fractions. ■, 293.15 K; □, 301.15 K; ▲, 303.15 K; △, 313.15 K; ◆, 323.15 K; ◇, 333.15 K; ●, 343.15 K.

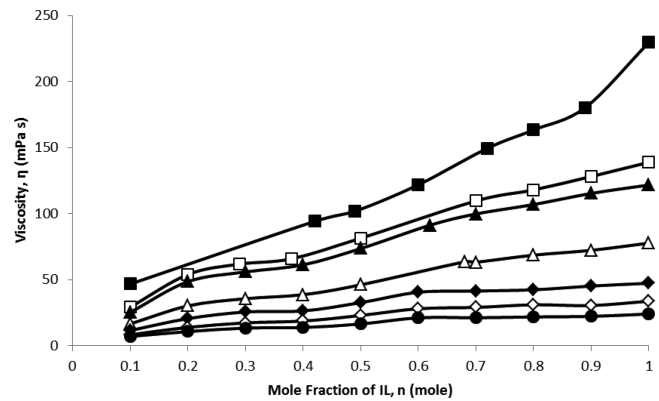


Figure 12. Experimental viscosities, η , of ternary mixtures [mmim][dmp]-MDEA-H₂O at different temperatures as a function of mole fractions. ■, 293.15 K; □, 301.15 K; ▲, 303.15 K; △, 313.15 K; ◆, 323.15 K; ◇, 333.15 K; ●, 343.15 K.

analysis. The obtained models after excluding nonsignificant model constants ($p > 0.05$), for [emim][dep]-MDEA-H₂O is

$$\begin{aligned} \ln \rho_{m,T} = & x_1 \ln \rho_{1,T} + x_2 \ln \rho_{2,T} + x_3 \ln \rho_{3,T} \\ & + 123.812 \left[\frac{x_1 x_2}{T} \right] - 431.999 \left[\frac{x_1 x_2 (x_1 - x_2)}{T} \right] \\ & + 299.190 \left[\frac{x_1 x_3}{T} \right] - 135.921 \left[\frac{x_2 x_3}{T} \right] \\ & - 1303.665 \left[\frac{x_2 x_3 (x_2 - x_3)}{T} \right] \end{aligned} \quad (2)$$

and for [mmim][dmp]-MDEA-H₂O is

$$\begin{aligned} \ln \rho_{m,T} = & x_1 \ln \rho_{1,T} + x_2 \ln \rho_{2,T} + x_3 \ln \rho_{3,T} \\ & + 92.957 \left[\frac{x_1 x_2}{T} \right] + 159.705 \left[\frac{x_1 x_2 (x_1 - x_2)}{T} \right] \\ & + 39.817 \left[\frac{x_1 x_3}{T} \right] + 106.868 \left[\frac{x_2 x_3}{T} \right] \end{aligned} \quad (3)$$

The calculated density values using eqs 2 and 3 against the experimental values are presented in Figures 14 and 15. The accuracy of the calculations was evaluated using absolute percentage error (APER) computed by

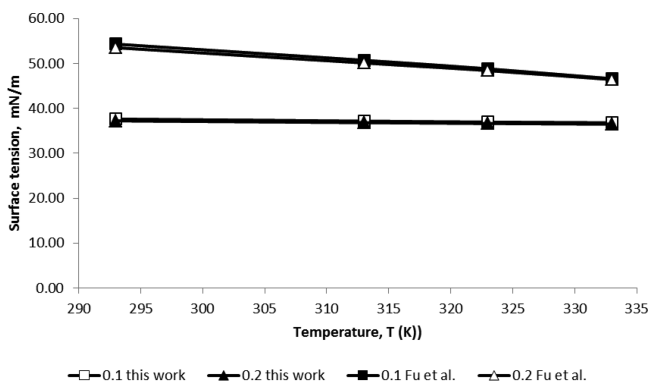


Figure 13. Comparison of experimental surface tension, γ between ternary mixtures [emim][dep]–MDEA–H₂O and MEA–MDEA–H₂O (Fu et al.³⁹) at different mole fractions as a function of temperature.

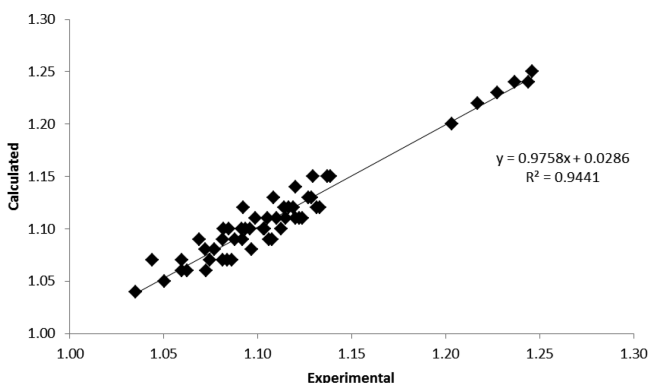


Figure 14. Density values of [emim][dep]–MDEA–H₂O calculated using eq 2 against the corresponding experimental values.

$$\text{APER} = \frac{100}{N} \sum \frac{|\text{Computed} - \text{Experimental}|}{\text{Experimental}} \quad (4)$$

The N in eq 4 is the number of data points in the data set. The APER for [emim][dep]–MDEA–H₂O is 0.8310 % in eq 2 and 1.2183 % for [mmim][dmp]–MDEA–H₂O in eq 3.

Surface Tension. The Jouyban–Acree model for representing the surface tension of ternary solvents is

$$\begin{aligned} \ln \gamma_{m,T} = & x_1 \ln \gamma_{1,T} + x_2 \ln \gamma_{2,T} + x_3 \ln \gamma_{3,T} \\ & + x_1 x_2 \sum_{j=0}^2 \left[\frac{A_j (x_1 - x_2)^j}{T} \right] + x_1 x_3 \\ & \times \sum_{j=0}^2 \left[\frac{B_j (x_1 - x_3)^j}{T} \right] + x_2 x_3 \sum_{j=0}^2 \left[\frac{C_j (x_2 - x_3)^j}{T} \right] \\ & + x_1 x_2 x_3 \sum_{j=0}^2 \left[\frac{D_j (x_1 - x_2 - x_3)^j}{T} \right] \end{aligned} \quad (5)$$

where $\gamma_{m,T}$, $\gamma_{1,T}$, $\gamma_{2,T}$, and $\gamma_{3,T}$ are the surface tensions of the mixture and solvents 1, 2, and 3 at temperature T , respectively, and D_j represent the model constants.⁴² These model constants are computed by regressing $(\ln \gamma_{m,T} - x_1 \ln \gamma_{1,T} - x_2 \ln \gamma_{2,T} - x_3 \ln \gamma_{3,T})$ against $x_1 x_2 / T$, $x_1 x_2 (x_1 - x_2) / T$, $x_1 x_2 (x_1 - x_2)^2 / T$, $x_1 x_3 / T$, $x_1 x_3 (x_1 - x_3) / T$, $x_1 x_3 (x_1 - x_3)^2 / T$, $x_2 x_3 / T$, $x_2 x_3 (x_2 - x_3) / T$, $x_2 x_3 (x_2 - x_3)^2 / T$, $x_1 x_2 x_3 / T$, $x_1 x_2 x_3 (x_1 - x_2 - x_3) / T$, and $x_1 x_2 x_3 (x_1 - x_2 - x_3)^2 / T$ using a no intercept least-squares analysis. The

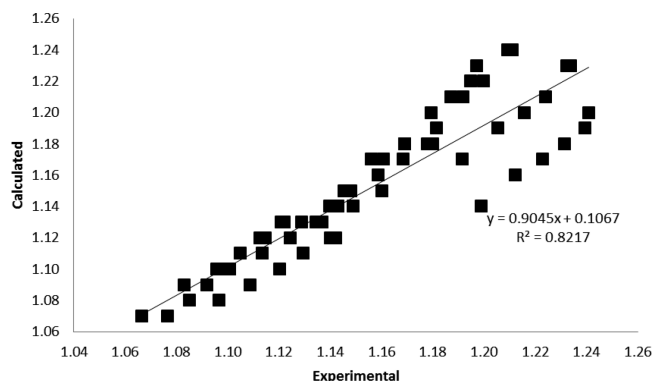


Figure 15. Density values of [mmim][dmp]–MDEA–H₂O calculated using eq 3 against the corresponding experimental values.

obtained models after excluding nonsignificant model constants ($p > 0.05$), for [emim][dep]–MDEA–H₂O is

$$\begin{aligned} \ln \gamma_{m,T} = & x_1 \ln \gamma_{1,T} + x_2 \ln \gamma_{2,T} + x_3 \ln \gamma_{3,T} - 184.940 \left[\frac{x_1 x_2}{T} \right] \\ & + 97.129 \left[\frac{x_1 x_2 (x_1 - x_2)}{T} \right] - 240.749 \left[\frac{x_1 x_3}{T} \right] \\ & + 268.683 \left[\frac{x_1 x_3 (x_1 - x_3)}{T} \right] - 608.197 \left[\frac{x_2 x_3}{T} \right] \\ & + 574.476 \left[\frac{x_2 x_3 (x_2 - x_3)}{T} \right] \end{aligned} \quad (6)$$

and for [mmim][dmp]–MDEA–H₂O is

$$\begin{aligned} \ln \gamma_{m,T} = & x_1 \ln \gamma_{1,T} + x_2 \ln \gamma_{2,T} + x_3 \ln \gamma_{3,T} - 171.909 \left[\frac{x_1 x_2}{T} \right] \\ & + 167.099 \left[\frac{x_1 x_2 (x_1 - x_2)}{T} \right] - 106.504 \left[\frac{x_1 x_3}{T} \right] \\ & - 500.764 \left[\frac{x_2 x_3}{T} \right] + 511.022 \left[\frac{x_2 x_3 (x_2 - x_3)}{T} \right] \end{aligned} \quad (7)$$

The calculated density values using eqs 6 and 7 against the experimental values are presented in Figures 16 and 17. The accuracy of the calculations was evaluated using absolute percentage error (APER) computed by eq 4, where N is the number of data points in the data set. The APER for [emim][dep]–MDEA–H₂O is 0.4858 % in eq 6 and 0.9032 % for [mmim][dmp]–MDEA–H₂O in eq 7.

Viscosity. The Jouyban–Acree model for representing the viscosity of ternary solvents is

$$\begin{aligned} \ln \eta_{m,T} = & x_1 \ln \eta_{1,T} + x_2 \ln \eta_{2,T} + x_3 \ln \eta_{3,T} \\ & + x_1 x_2 \sum_{j=0}^2 \left[\frac{A_j (x_1 - x_2)^j}{T} \right] + x_1 x_3 \\ & \times \sum_{j=0}^2 \left[\frac{B_j (x_1 - x_3)^j}{T} \right] + x_2 x_3 \sum_{j=0}^2 \left[\frac{C_j (x_2 - x_3)^j}{T} \right] \\ & + x_1 x_2 x_3 \sum_{j=0}^2 \left[\frac{D_j (x_1 - x_2 - x_3)^j}{T} \right] \end{aligned} \quad (8)$$

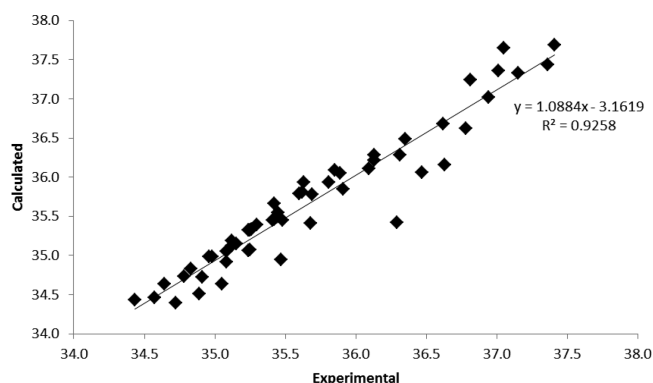


Figure 16. Surface tension values of [emim][dep]-MDEA-H₂O calculated using eq 6 against the corresponding experimental values.

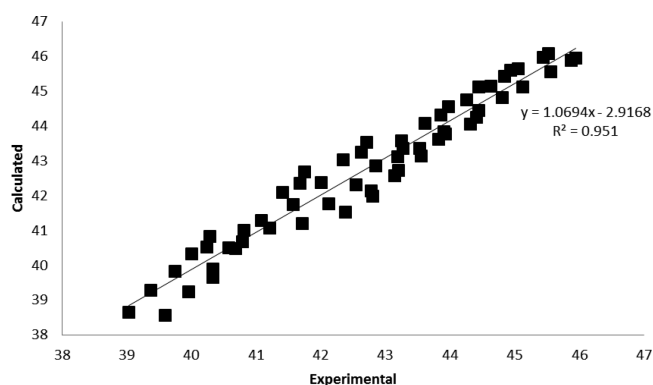


Figure 17. Surface tension values of [mmim][dmp]-MDEA-H₂O calculated using eq 7 against the corresponding experimental values.

where $\eta_{m,T}$, $\eta_{1,T}$, $\eta_{2,T}$, and $\eta_{3,T}$ are the viscosities of the mixture and solvents 1, 2, and mixed solvents with respect to solvent composition and temperature by using Jouyban-Acree model.^{43,44} These model constants are computed by regressing $(\ln \eta_{m,T} - x_1 \ln \eta_{1,T} - x_2 \ln \eta_{2,T} - x_3 \ln \eta_{3,T})$ against x_1x_2/T , $x_1x_2(x_1 - x_2)/T$, $x_1x_2(x_1 - x_2)^2/T$, x_1x_3/T , $x_1x_3(x_1 - x_3)/T$, $x_1x_3(x_1 - x_3)^2/T$, x_2x_3/T , $x_2x_3(x_2 - x_3)/T$, $x_2x_3(x_2 - x_3)^2/T$, $x_1x_2x_3/T$, $x_1x_2x_3(x_1 - x_2 - x_3)/T$, and $x_1x_2x_3(x_1 - x_2 - x_3)^2/T$ using a no intercept least-squares analysis. The obtained models after excluding nonsignificant model constants ($p > 0.05$), for [emim][dep]-MDEA-H₂O is

$$\begin{aligned} \ln \eta_{m,T} = & x_1 \ln \eta_{1,T} + x_2 \ln \eta_{2,T} + x_3 \ln \eta_{3,T} \\ & + 630.494 \left[\frac{x_1x_2}{T} \right] - 2015.538 \left[\frac{x_1x_2(x_1 - x_2)}{T} \right] \\ & + 2973.430 \left[\frac{x_1x_3}{T} \right] + 2354.561 \left[\frac{x_1x_3(x_1 - x_3)}{T} \right] \\ & - 3066.373 \left[\frac{x_2x_3}{T} \right] - 10617.4 \left[\frac{x_2x_3(x_2 - x_3)}{T} \right] \end{aligned} \quad (9)$$

and for [mmim][dmp]-MDEA-H₂O is

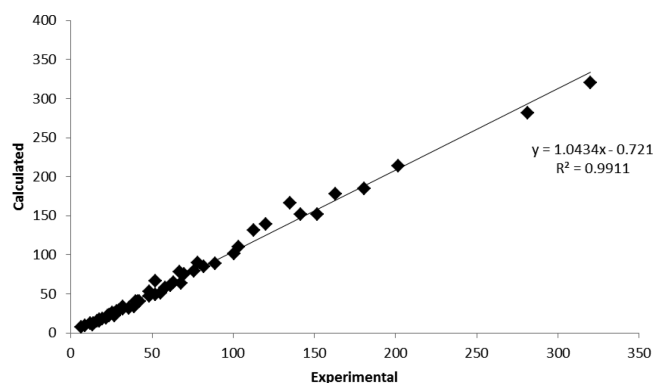


Figure 18. Viscosity values of [emim][dep]-MDEA-H₂O calculated using eq 9 against the corresponding experimental values.

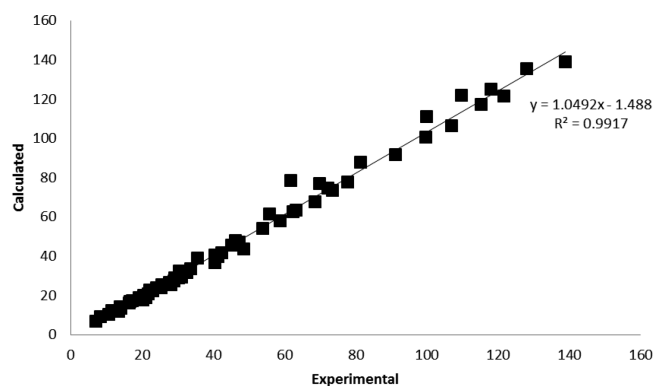


Figure 19. Viscosity values of [mmim][dmp]-MDEA-H₂O calculated using eq 10 against the corresponding experimental values.

$$\begin{aligned} \ln \eta_{m,T} = & x_1 \ln \eta_{1,T} + x_2 \ln \eta_{2,T} + x_3 \ln \eta_{3,T} \\ & + 71.289 \left[\frac{x_1x_2}{T} \right] + 2581.633 \left[\frac{x_1x_2(x_1 - x_2)}{T} \right] \\ & - 1651.581 \left[\frac{x_1x_3}{T} \right] + 1541.061 \left[\frac{x_1x_3(x_1 - x_3)}{T} \right] \\ & - 2048.221 \left[\frac{x_2x_3}{T} \right] - 2800.601 \left[\frac{x_2x_3(x_2 - x_3)}{T} \right] \end{aligned} \quad (10)$$

The calculated density values using eqs 9 and 10 against the experimental values are presented in Figures 18 and 19. The accuracy of the calculations was evaluated using absolute percentage error (APER) computed by eq 4, which N is the number of data points in the data set. The APER for [emim][dep]-MDEA-H₂O is 7.0278 % in eq 9 and 4.4109 % for [mmim][dmp]-MDEA-H₂O in eq 10.

4. CONCLUSION

Aqueous ternary mixtures of [emim][dep] and [mmim][dmp] with MDEA were prepared and their physicochemical properties namely densities, ρ , surface tensions, γ , and viscosities, η , in the temperature range from (293.15 to 343.15) K were measured and reported. The ternary mixtures demonstrate temperature-dependent behaviors. Densities and surface tensions of mixtures decreased linearly with temperature, meanwhile viscosities decreased nonlinearly. The accuracy assessment of densities, surface tensions, and viscosities was completed by correlation. The best correlation for density and surface tension data are

linear equation, and polynomial equation for viscosity. The experimental density, surface tension and viscosity also influenced by mole fractions of ILs. This article enlarges widely the experimental physicochemical properties information about ILs–MDEA–H₂O systems as it includes the behavior at various temperatures commonly found in engineering process. The proposed models provided reasonable accurate results to calculate the density, surface tension and viscosity of ILs–MDEA–H₂O mixtures with respect to their composition and temperature. The overall APER for density, surface tension and viscosity of [emim][dep]–MDEA–H₂O and [mmim][dmp]–MDEA–H₂O are below than 8 %, revealing that the Jouyban–Acree model is able to accurately represent the physicochemical properties data.

AUTHOR INFORMATION

Corresponding Author

*E-mail: asrina@um.edu.my. Tel: +603-79675160. Fax: +603-79677188.

Funding

The authors gratefully acknowledge the University Malaya Research Grant UMRG (RP006F-13SUS), UMRG-CO₂ (RP015/2012A), and BK003-2012 for the financial support.

Notes

The authors declare no competing financial interest.

ACKNOWLEDGMENTS

A special thank you goes to Prof. Dr. Abolghasem Jouyban and his research group from Drug Applied Research Center and Faculty of Pharmacy, Tabriz University of Medical Sciences, Iran for sharing their knowledge and helping in Jouyban–Acree model correlation analysis of the ternary systems. Our sincere appreciation is also extended to University of Malaya Centre of Ionic Liquid (UMCIL).

REFERENCES

- (1) Aschenbrenner, O.; Styring, P. Comparative study of solvent properties for carbon dioxide absorption. *Energy Environ. Sci.* **2010**, *3*, 1106–1113.
- (2) Chiesa, P.; Consonni, S. P. Shift reactors and physical absorption for low-CO₂ emission IGCCs. *J. Eng. Gas Turbines Power* **1999**, *121*, 295–305.
- (3) Sairi, N. A.; Yusoff, R.; Alias, Y.; Aroua, M. K. Solubilities of CO₂ in aqueous *N*-methyldiethanolamine and guanidinium trifluoromethanesulfonate ionic liquid systems at elevated pressures. *Fluid Phase Equilib.* **2011**, *300* (1–2), 89–94.
- (4) Rochelle, G. T. Amine scrubbing for CO₂ capture. *Science* **2009**, *325*, 1652–1654.
- (5) Aroonwilas, A.; Veawab, A. Characterization and comparison of the CO₂ absorption performance into single and blended alkanolamines in a packed column. *Ind. Eng. Chem. Res.* **2004**, *43*, 2228–2237.
- (6) Chang, F. Y.; Chao, K. J.; Cheng, H. H.; Tan, C. S. Adsorption of CO₂ onto amine-grafted mesoporous silicas. *Sep. Purif. Technol.* **2009**, *70*, 87–95.
- (7) Powell, C. E.; Qiao, G. G. Polymeric CO₂/N₂ gas separation membranes for the capture carbon dioxide from power plant flue gases. *J. Membr. Sci.* **2006**, *279*, 1–49.
- (8) Holbrey, J. D.; Reichert, W. M.; Swatoski, R. P.; Broker, G. A.; Pitner, W. R.; Seddon, K. R.; Rogers, R. D. Efficient, halide free synthesis of new, low cost ionic liquids: alkylimidazolium salts containing methyl- and ethyl- sulfate anions. *Green Chem.* **2002**, *4*, 407–413.
- (9) Wang, J.; Wang, D.; Li, Z.; Zhang, F. Vapor pressure measurement and correlation or prediction for water, 1-propanol, 2-propanol, and their binary mixtures with [MMIM][DMP] ionic liquid. *J. Chem. Eng. Data* **2010**, *55*, 4872–4877.
- (10) Yu, C. H.; Cheng, H. H.; Tan, C. S. CO₂ capture by alkanolamines solutions containing diethylenetriamine and piperazine in a rotating packed bed. *Int. J. Greenhouse Gas Control* **2012**, *9*, 136–147.
- (11) Wang, Y. T.; Fang, C. G.; Zhang, F. The performance of CO₂ absorption in mixed aqueous solution of MDEA and amino acid ionic liquid. *CIESC J.* **2009**, *60*, 2781–2786.
- (12) Zang, F.; Ma, J. W. M.; Zhou, Z.; Wu, Y. T.; Zhang, Z. B. Study on the absorption of carbon dioxide in high concentrated MDEA and ILs solutions. *Chem. Eng. J.* **2012**, *181*–182, 222–228.
- (13) Gao, Y.; Zhang, F.; Huang, K.; Ma, J. W.; Wu, Y. T.; Zhang, Z. B. Absorption of CO₂ in amino acid ionic liquid (AAIL) activated MDEA solutions. *Int. J. Greenhouse Gas Control* **2013**, *19*, 379–386.
- (14) Ahmady, A.; Hashim, M. A.; Aroua, M. K. Absorption of carbon dioxide in the aqueous mixtures of methyldiethanolamine with three types of imidazolium-based ionic liquids. *Fluid Phase Equilib.* **2011**, *309*, 76–82.
- (15) Soriano, A. N.; Doma, B. T., Jr.; Li, M.-H. Density and refractive index measurements of 1-ethyl-3-methylimidazolium-based ionic liquids. *J. Taiwan Inst. Chem. E* **2010**, *41*, 115–121.
- (16) Wilkes, J. S. Properties of ionic liquid solvents for catalysis. *J. Mol. Catal. A: Chem.* **2004**, *214*, 11–17.
- (17) Brennecke, J. F.; Maginn, E. J. Ionic liquids: Innovative fluids for chemical processing. *AIChE J.* **2001**, *47* (11), 2384–2389.
- (18) Iglesias-Otero, M. A.; Troncoso, J.; Carballo, E.; Romani, L. Density and refractive index in mixtures of ionic liquids and organic solvents: Correlations and predictions. *J. Chem. Thermodyn.* **2008**, *40*, 949–956.
- (19) Kurnia, K. A.; Mutalib, M. I. A. Densities and viscosities of binary mixture of the ionic liquid bis(2-hydroxyethyl)ammonium propionate with methanol, ethanol and 1-propanol at T = (293.15, 303.15, 313.15 and 323.15) K and at P = 0.1 MPa. *J. Chem. Eng. Data* **2011**, *56*, 79–83.
- (20) Troncoso, J.; Cerdeirina, C. A.; Sanmamed, Y. A.; Romani, L.; Rebelo, L. P. N. Thermodynamic properties of imidazolium-based ionic liquids: Densities, heat capacities and enthalpies of fusion of [bmim][PF₆] and [bmim][NTf₂]. *J. Chem. Eng. Data* **2006**, *51* (5), 1856–1859.
- (21) Kolbeck, C.; Lehmann, J.; Lovelock, K. R. J. Density and surface tension of ionic liquids. *J. Phys. Chem. B* **2010**, *11*, 17025–17036.
- (22) Zhao, Y.; Zhang, X.; Zeng, S.; Zhou, Q.; Dong, H.; Tian, X.; Zhang, S. Viscosity and performances of carbon dioxide capture in 16 absorbents of amine+ionic liquid+H₂O, ionic liquid+H₂O and amine+H₂O systems. *J. Chem. Eng. Data* **2010**, *55*, 3513–3519.
- (23) Ahmady, A.; Hashim, M. A.; Aroua, M. K. Experimental investigation on the solubility and initial rate of absorption of CO₂ in aqueous mixtures of methyldiethanolamine with the ionic liquid 1-butyl-3-methylimidazolium tetrafluoroborate. *J. Chem. Eng. Data* **2010**, *55* (12), 5733–5738.
- (24) Akbar, M. M.; Murugesan, T. Thermophysical properties of 1-hexyl-3-methylimidazolium tetrafluoroborate [hmim][BF₄] + *N*-methyldiethanolamine (MDEA) at temperatures (303.15 to 323.15 K). *J. Mol. Liq.* **2013**, *177*, 54–59.
- (25) Aguila-Hernandez, J.; Trejo, A.; Garcia-Flores, B. E. Surface tension and foam behaviour of aqueous solutions of blends of three alkanolamines, as a function of temperature. *Colloids Surf., A* **2007**, *308*, 33–46.
- (26) Bernal-Garcia, J. M.; Ramos-Estrada, M.; Iglesias-Silva, G. A.; Hall, K. R. Densities and excess molar volumes of aqueous solutions of *n*-methyldiethanolamine (MDEA) at temperatures (283.15 to 363.15) K. *J. Chem. Eng. Data* **2003**, *48*, 1442–1445.
- (27) Alvarez, E.; Rendo, R.; Sanjurjo, B.; Sanchez-Vilas, M.; Navaza, J. M. Surface tension of binary mixtures of water + *N*-methyldiethanolamine and ternary mixtures of this amine and water with monoethanolamine, diethanolamine, and 2-amino-2-methyl-1-propanol from 25 to 50 °C. *J. Chem. Eng. Data* **1998**, *43*, 1027–1029.
- (28) Al-Ghawas, H. A.; Hagewiesche, D. P.; Ruiz-Ibanez, G.; Sandall, O. C. Physicochemical properties important for carbon dioxide absorption in aqueous methyldiethanolamine. *J. Chem. Eng. Data* **1989**, *34* (4), 385–391.

- (29) Ciocirlan, O.; Croitoru, O.; Iulian, O. Densities and viscosities for binary mixtures of 1-butyl-3-methylimidazolium tetrafluoroborate ionic liquid with molecular solvents. *J. Chem. Eng. Data* **2011**, *56*, 1526–1534.
- (30) Soriano, A. N.; Doma, B. T., Jr.; Li, M.-H. Measurements of the density and refractive index for 1-*n*-butyl-3-methylimidazolium-based ionic liquids. *J. Chem. Eng. Data* **2009**, *41*, 301–307.
- (31) Jacquemin, J.; Ge, R.; Nancarrow, P.; Rooney, D. W.; Costa-Gomes, M. F.; Padua, A. A. H.; Hardcare, C. Prediction of ionic liquid properties. I. Volumetric properties as a function of temperature at 0.1 MPa. *J. Chem. Eng. Data* **2008**, *53*, 716–726.
- (32) Rodriguez, H.; Brennecke, J. F. Temperature and composition dependence on the density and viscosity of binary mixtures of water + ionic liquid. *J. Chem. Eng. Data* **2006**, *51*, 2145–2155.
- (33) Wang, J. Y.; Jiang, H. C.; Liu, Y. M.; Hu, Y. Q. Density and surface tension of pure 1-ethyl-3-methylimidazolium L-lactate ionic liquid and its binary mixtures with water. *J. Chem. Thermodyn.* **2011**, *43*, 800–804.
- (34) Tariq, M.; Freire, M. G.; Saramago, B.; Coutinho, J. A. P.; Lopes, J. N. C.; Rebelo, L. P. N. Surface tension of ionic liquid and ionic liquid solutions. *Chem. Soc. Rev.* **2012**, *41* (2), 829–868.
- (35) Carvalho, P. J.; Freire, M. G.; Marrucho, I. M.; Queimada, A. J.; Coutinho, J. A. P. *J. Chem. Eng. Data* **2008**, *53*, 1346–1350.
- (36) Ochedzan-Siodlak, W.; Dziubek, K.; Siodlak, D. Densities and viscosities of imidazolium and pyridinium chloroaluminate ionic liquids. *J. Mol. Liq.* **2013**, *177*, 85–93.
- (37) Baroutian, S.; Aroua, M. K.; Raman, A. A. A.; Sulaiman, M. N. S. Viscosities and densities of binary and ternary blends of palm oil + palm biodiesel + diesel fuel at different temperatures. *J. Chem. Eng. Data* **2010**, *55*, 504–507.
- (38) Domanska, U.; Laskowska, M. Effect of temperature and composition on the density and viscosity of binary mixtures of ionic liquid with alcohols. *J. Solution Chem.* **2009**, *38*, 779–799.
- (39) Fu, D.; Wei, L.; Liu, S. Experiment and model for the surface tension of carbonated MEA-MDEA aqueous solutions. *Fluid Phase Equilib.* **2013**, *337*, 83–88.
- (40) Jouyban, A.; Fathi-Azarbayjani, A.; Khoubnasabjafari, M.; Acree, W. E., Jr. Mathematical representation of the density of liquid mixtures at various temperatures using Jouyban-Acree model. *Indian J. Chem.* **2005**, *44A*, 1–8.
- (41) Jouyban, A.; Maljaeib, S. H.; Khoubnasabjafari, M.; Fathi-Azarbayjani, A.; Acree, W. E., Jr. A global model to predict density of non-aqueous binary solvent mixtures at various temperatures. *Indian J. Chem.* **2012**, *51A*, 695–698.
- (42) Jouyban, A.; Fathi-Azarbayjani, A.; Acree, W. E., Jr. Surface tension calculation of mixed solvents with respect to solvent composition and temperature by using Jouyban-Acree model. *Chem. Pharm. Bull.* **2004**, *52*, 1219–1222.
- (43) Jouyban, A.; Khoubnasabjafari, M.; Vaez-Gharamaleki, Z.; Fekari, Z.; Acree, W. E., Jr. Calculation of the viscosity of binary liquids at various temperatures using Jouyban-Acree model. *Chem. Pharm. Bull.* **2005**, *53* (5), 519–523.
- (44) Jouyban, A.; Soleymani, J.; Jafari, F.; Khoubnasabjafari, M.; Acree, W. E. Mathematical Representation of Viscosity of Ionic Liquid + Molecular Solvent Mixtures at Various Temperatures Using the Jouyban-Acree Model. *J. Chem. Eng. Data* **2013**, *58*, 1523–1528.